

# UC Davis

## UC Davis Previously Published Works

### Title

Timing is Everything: Optimizing load flexibility of heat pump water heaters for cost, comfort, and carbon emissions

### Permalink

<https://escholarship.org/uc/item/299944qn>

### Authors

Mande, Caton  
Aboud, Aref  
dela Rosa, Loren  
et al.

### Publication Date

2022-08-01

Peer reviewed

# Timing is everything: Optimizing load flexibility of heat pump water heaters for cost, comfort, and carbon emissions

*Caton Mande, UC Davis Western Cooling Efficiency Center*  
*Aref Aboud, UC Davis Western Cooling Efficiency Center*  
*Loren dela Rosa, UC Davis Chemical Engineering*  
*Rachael Collins, UC Davis Western Cooling Efficiency Center*  
*Matthew J. Ellis, UC Davis Chemical Engineering*

## ABSTRACT

As California continues to decarbonize the electrical grid and more customers electrify, load flexibility among heat pumps is becoming critical for maximizing the use of carbon-free electricity sources, stabilizing the electricity grid, and minimizing operating costs to end-users. The transition to all-electric housing has many concerned about potential increases in utility costs. Load flexibility controls offer a way to mitigate the impact of electrification on customers by shifting consumption to times of day with lower rates without compromising their comfort. Heat pump water heaters (HPWHs) are currently controlled using rule-based logic to maintain a programmed water temperature setpoint. This type of control usually does not provide any flexibility to when the heat pump operates. Economic model predictive control (MPC) is an advanced control technique that can provide automated load flexibility due to its ability to account for time-varying electric tariffs and available energy storage. A new configurable control framework is motivated and described to address the challenges of configuring economic MPC for deployment. This framework utilizes a graph-based system representation of the physical system that automatically instantiates the underlying economic MPC problem from the system representation and requires minimum MPC expertise. In this work, the MPC framework is described and applied to a simulated HPWH. The closed-loop simulation results are compared to the results obtained from simulations of an HPWH under a rule-based control approach.

## Introduction

With California's ambitious goal of achieving 100% carbon-free electricity by 2045 (CEC 2022), the benefits of electrification are likely to grow in the future as the electric grid continues to be decarbonized. With water heating accounting for the second-largest energy end use in U.S. homes (EIA 2018), several state-programs are incentivizing homeowners with natural-gas water heaters to switch to more energy efficient heat pump water heaters (HPWHs) that can be powered by renewable energy sources (CPUC 2020). Most HPWHs are controlled using rule-based logic to maintain a programmed water temperature setpoint. While this approach is proven and robust for maintaining a user-defined setpoint, this type of control usually does not provide any flexibility as to when the HPWH operates — the HPWH is turned on until it reaches the setpoint, regardless of the electricity cost or grid GHG emissions rate.

HPWHs can achieve load flexibility by using available thermal storage (through the built-in storage tank) to shift electricity use away from peak hours by storing hot water generated with low-cost, emissions-free renewable electricity for use later in the day (Delforge 2020). For example, it can result in heating water to higher temperatures, part of the time, to prevent heating

during peak hours. However, pre-heating water is not perfect and some of that heat can be lost to the ambient environment. Thus, sophisticated control strategies are needed to balance thermal storage and efficiency losses of HPWHs (Delforge and Vukovich 2018).

Model predictive control (MPC) is an optimization-based predictive control technique that determines control actions by predicting system behavior over a horizon and choosing the control actions that optimizes a cost function (Rawlings, Mayne, and Diehl 2019). The main advantage of MPC over other control approaches is that performance considerations and constraints are explicitly addressed in its formulation. Economic MPC is a specific type of MPC that uses an economic cost function, making it ideal for controlling and optimizing energy systems (Ellis, Durand, and Christofides 2014). For example, with a time-varying electric tariff, economic MPC may be used to determine the optimal operation of energy systems, accounting for forecasts of the ambient temperature, electric tariff, system heat gains/losses, and occupant demand or comfort. MPC can also account for available thermal energy storage to shape heat pump load.

Several works have used MPC for HPWH load flexibility. Wanjiru, Sichilalu and Xia (2017) developed an MPC strategy to operate both a HPWH and less energy-efficient electric powered instant shower for domestic hot water demand. The MPC was able to operate both heating devices during the cheaper time-of-use periods and prioritized the use of the HPWH over the instant shower. Jin and Christensen (2014) proposed an MPC framework to find optimal setpoints for a HPWH to maximize energy savings and thermal comfort. Considerable cost and energy savings were achieved with only a slight decrease in thermal comfort.

In general, setting up, configuring, and deploying MPC for energy systems is a practical challenge because it has many components (e.g., a data collector, data storage, external data sources, a programmatic view of the system, and an optimization solver). Although software packages exist to express and solve MPC problems, these packages tend to programmatically represent physical systems (i.e., HP systems) as a single monolithic entity even though systems are usually comprised of several subsystems. This monolithic representation limits the re-use of subcomponents from one deployment to another. As a result, an MPC expert is required to create a new or reconfigure an existing representation for each new system.

To this end, the objective of the present work is to create a configurable framework for representing HPWHs. The physical system is programmatically represented as a directed graph, which may be created by a non-MPC expert. After the system representation is created, external data sources can be configured, and the resulting MPC problem can be automatically created and solved for closed-loop control of the system. The benefit of the proposed system representation is that systems may be expressed as a few object types, which aids modularity and reduces the level of MPC expertise needed to deploy an MPC system. This framework is applied to a simulated HPWH and is compared against rule-based control to demonstrate the approach.

## **Review of Economic Model Predictive Control**

Economic MPC, referred to as MPC for simplicity in the remainder of the paper, is an implicit control law constructed by repeatedly solving an optimal control problem. A general MPC optimal control problem is given in Equation 1 and has two parts: the cost function and the constraints. One main difference between MPC and other feedback control approaches (e.g., proportion-integral control) is that MPC accounts for future system behavior and expected costs. This ensures that the MPC does not make myopic control decisions. In Equation 1, the stage cost function is denoted by  $l_e(\cdot)$  where the subscript  $e$  is used to emphasize that the stage cost is

economic. The accumulated stage costs over the prediction horizon are minimized in the optimal control problem and subject two five constraints. The first constraint in Equation 1 is the system model that describes the relationship between the system states, manipulated inputs, and exogenous inputs. Here, the dynamic model is assumed to be a linear time-varying model – the form needed for the HPWH application – but other types of dynamic models may be used. The second constraint represents any inequality or equality constraint that depends on the states and/or inputs. Since exogenous inputs may vary with time, these inputs are generated by external forecasting models and used to predict the system behavior over the prediction horizon. The remaining three constraints apply to the initial state as well as the upper and lower bounds for both the manipulated input and the states.

In Equation 1, the notation  $\mathbf{u}$  denotes the sequence of input values that are the decision variables of the optimization problem (i.e.,  $\mathbf{u} := \{u_0, \dots, u_{N-1}\}$ ). The optimal sequence of inputs that minimizes the cost function in Equation 1 is denoted by  $\mathbf{u}^* := \{u_0^*, \dots, u_{N-1}^*\}$ .

Equation 1: MPC optimal control problem

$$\begin{aligned} & \min_{\mathbf{u}} \sum_{k=0}^{N-1} l_e(x_k, u_k, d_k) \\ & \text{subject to} \\ & \quad x_{k+1} = A_k x_k + B_k u_k + B_{d,k} d_k \\ & \quad lb \leq G x_k + H \begin{bmatrix} u_k \\ d_k \end{bmatrix} \leq ub \\ & \quad x_0 = \hat{x} \\ & \quad u_{lb,k} \leq u_k \leq u_{ub,k} \\ & \quad x_{lb,k+1} \leq x_{k+1} \leq x_{ub,k+1}, \quad k = 0, \dots, N - 1 \end{aligned}$$

where,

$N$  is the number of time steps in the prediction horizon,

$x_k$  is the system state at the  $k$ th time step in the prediction horizon,

$u_k$  is the manipulated input at the  $k$ th time step in the prediction horizon,

$d_k$  is the time-varying exogenous input at the  $k$ th time step in the prediction horizon,

$A_k, B_k, B_{d,k}, G,$  and  $H$  are matrices of appropriate dimensions,

$lb$  and  $ub$  are vectors of appropriate dimensions,

$\hat{x}$  is the measured or estimated state at the current time, and

$u_{lb,k}, x_{lb,k}, u_{ub,k},$  and  $x_{ub,k}$  are the lower and upper bounds on the inputs and states at the  $k$ th time step, respectively.

MPC is implemented according to a receding horizon implementation where real-time is partitioned into discrete sample times. At each sample time, the MPC receives the current state measurement or estimate and forecasts of all exogenous inputs. Next, an instance of the optimal control problem (Equation 1) is created and solved to compute the optimal input sequence ( $\mathbf{u}^*$ ). The first element in the sequence ( $u_0^*$ ) is sent to the system to be implemented until the next sample time. At the next sample time, the MPC receives an updated state measurement or estimate and an updated forecast of all exogenous inputs and solves for the next optimal input sequence.

## MPC Framework with a Graph-based System Representation

The formulation of MPC in Equation 1 is usually created by an MPC expert, who formulates the stage cost for a specific application and specifies the system model in a monolithic manner. For many energy system applications such as HPWHs, requiring an MPC expert to configure MPC for each application is not scalable. Instead, a framework that enables easy configuration of the MPC and does not require an MPC expert is needed. One objective of the present work is to create a configurable framework for representing energy system problems. In the proposed framework, the physical system is programmatically represented as a directed graph, which may be created by a non-MPC expert. After the system representation is created, external data sources can be configured, and the resulting MPC problem (Equation 1) can be automatically created and solved for closed-loop control of the system.

### Directed Graph System Representation

A directed graph consists of a set of nodes or vertices connected by directed arcs or edges. Directed graphs serve as a natural structure for the digital representation of a system comprised of many components and subsystems since the directed edges can symbolize the flow of resource, such as energy, material, or information, in a single direction and system components, costs, and exogenous inputs can be represented by the vertices. The proposed system representation describes the system (model and constraints) along with the cost and is modular. This enables the re-use of objects that map the physical world to a digital representation of the system. The directed graph system representation includes three vertex types: source, sink, and system. Each vertex contains the information necessary to create the MPC problem.

A source vertex represents an available supply of resources with a cost associated with consumption. The decision variable associated with a source is the amount of the resource to purchase. It only has one outgoing edge, representing the total outflow of the resource. A source vertex can represent, for example, an electric or water utility or a penalty associated with not meeting hot water demand.

A sink vertex represents an exogenous input that does not change based on the optimization problem. It only has ingoing edges and can be used to represent, for example, the hot water demand or outdoor air temperature. The associated data is the predicted exogenous input values over the prediction horizon, which could be provided from an external application programming interface (API) or a forecasting model. While the sinks provide input data to create the MPC problem, it can be loosely interpreted as representing an outflow of a resource from the system, therefore, no decision variables or constraints are associated with a sink.

The system vertex represents a component of the system that can be manipulated or influenced by MPC. It has ingoing and outgoing edges that specify an equality relationship between variables of different vertices. The system vertex has a static or dynamic mathematical model which defines any relationship between the variables (internal or from edges) and the constraints that the variables must satisfy.

The goal is to keep the vertices general so the representation can be extended beyond HPWHs to other energy systems. For example, the system vertex type includes the following data: variable identifiers, model, requirements, and the ingoing and outgoing edges. Through this programmatic representation, the variable identifiers are used to create optimization variables associated with the vertex and facilitate the transmission of the optimal decision variable solutions computed by the external solver back to the system representation.

To describe how the system representation is automatically transcribed to the MPC problem in Equation 1, let  $\mathcal{S}$  be the set of source vertices,  $\mathcal{D}$  be the set of sink vertices,  $\mathcal{V}$  be the set of system vertices,  $p_s(k)$  be the prices of source  $s \in \mathcal{S}$  at the  $k$ th time step,  $u_s(k)$  be the amount of resource  $s \in \mathcal{S}$  purchased,  $\tilde{d}_j(k)$  be the predicted value of the  $j$ th sink at the  $k$ th time step ( $j \in \mathcal{D}$ ),  $x_v(k)$ ,  $u_v(k)$ , and  $\tilde{d}_v(k)$  be the state, manipulated input, and exogenous input, respectively, for the  $v$ th vertex at the  $k$ th time step ( $v \in \mathcal{V}$ ). For a given system representation, the associated MPC optimal control problem is given by Equation 2.

Equation 2: MPC optimal control problem generated from the system representation

$$\begin{aligned} & \min_{\mathbf{u}} \sum_{k=0}^{N-1} \sum_{s \in \mathcal{S}} p_s(k) u_s(k) \\ & \text{subject to} \\ & x_{v,k+1} = A_{v,k} x_{v,k} + B_{v,k} u_{v,k} + B_{v,d,k} \tilde{d}_{v,k}, \\ & lb_v \leq G_v x_{v,k} + H_v \begin{bmatrix} u_{v,k} \\ \tilde{d}_{v,k} \end{bmatrix} \leq ub_v \\ & x_{v,0} = \hat{x}_v, \forall v \in \mathcal{V} \\ & u_{lb,k} \leq u_k \leq u_{ub,k} \\ & x_{lb,k+1} \leq x_{k+1} \leq x_{ub,k+1}, \quad k = 0, \dots, N-1 \end{aligned}$$

where the parts of problem are analogous to that in Equation 1 and  $x_k$  and  $u_k$  are vectors representing a concatenation of all states and inputs, respectively.

## Overall MPC Framework

The directed graph is one subcomponent of the overall MPC framework as seen in Figure 1. First, the system graph is configured for a particular application [label (1)]. After the system graph is configured, the overall MPC can be used for real-time control and optimization. In this framework, data access objects are used to load timeseries data from a timeseries database, which can be populated from external data sources [label (2)]. Once the system graph is populated with necessary timeseries data, the system graph is fed to an optimization problem factory [label (3)] in which an instance of the MPC problem is created that takes the form of Equation 2 and is solved using an optimization solver [label (4)]. The optimal decision is mapped to the system graph [label (5)] and sent to the data access objects to write the solution to the database [label (6)].

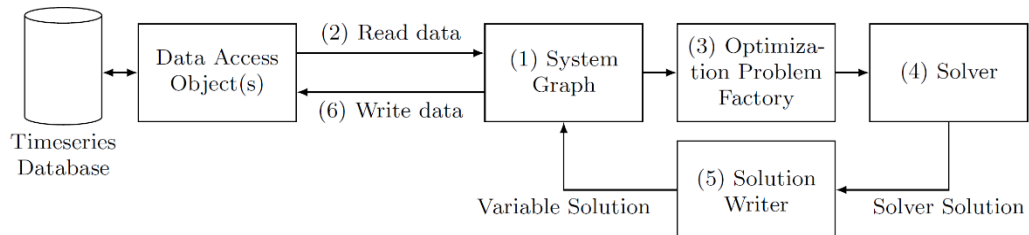


Figure 1: MPC Framework Design Incorporating the System Graph

The present work is focused on implementing the MPC framework on devices that are Wi-Fi-enabled and have an application programming interface that allows runtime or setpoints to

be controlled. However, the research team believes that manufacturers or third-party companies could use the framework as the original equipment manufacturer control or a retrofittable control.

## **Application of the MPC Framework to Heat Pump Water Heaters**

In this section, the MPC framework is applied to a HPWH system. A single-tank 240 Volt HPWH system providing hot water to a single-family home is considered. The HPWH has a nominal capacity of 65 gallons and rated capacity of 59 gallons. The heat pump (HP) compressor consumes electrical energy to move heat from the surrounding garage or utility closet air into the storage tank through the vapor compression cycle. If the HP is unable to meet the current load, an upper and lower electric resistance heating element may be turned on to quickly heat the tank water. The hot water in the storage tank is consumed by the occupant. The tank outlet has a mixing valve that mixes the tank hot water with cold tap water to meet a desired temperature setpoint. The mixing valve enables heating the tank above the desired hot water temperature, however, maintaining the tank temperature within a pre-specified minimum and maximum temperature is desired.

### **Directed Graph System Representation for Heat Pump Water Heaters**

Figure 2 shows the directed graph representation for the HPWH system. Four system vertices are needed to describe the problem:

- (1) describing the storage tank thermal dynamics and its associated constraints,
- (2) -(3) describing the efficiency relationship of the heat pump and resistive heater,
- (4) describing the relationship between total power consumption of the HPWH and the power consumption of the HP and electric resistive heaters.

The sources include marginal grid GHG emissions, electric utility, and temperature violation. The forecasted marginal grid GHG emissions is provided through an external data source. The electric utility considered uses a time-of-use (TOU) electric rate profile. The temperature violation is a penalty for violating the minimum and maximum water temperature within the storage tank. Although this penalty does not have a physical interpretation, it results in a soft constraint of the minimum and maximum temperature bounds to prevent the optimization problem becoming infeasible when it is not possible to keep the water temperature within the bounds.

The sinks represent the exogenous inputs that do not depend on the decisions of the optimization problem. In the HPWH system, the ambient temperature is predicted from the outdoor air temperature forecast obtained through an external weather source. The ambient temperature is the primary driver for heat loss from the tank and after future refinements will affect the heat pump efficiency. The cold-water inlet temperature of make-up tap water is another sink in the HPWH system. While this temperature varies throughout the day and over the year, it is taken to be a constant value, since a model that forecasts its value over the year is currently unavailable. Because of the framework design, other prediction models for this temperature could be further explored if needed for future refinement. The hot water demand or hot water flow rate is the last sink. The predictor will account for potential time-of-day and day-type variability of hot water consumption.

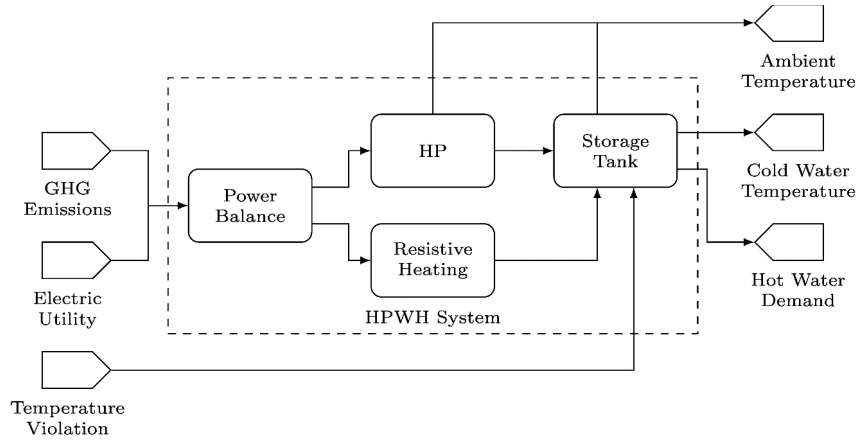


Figure 2: Directed Graph System Representation of the HPWH

### Simulation Setup

The performance of the MPC is evaluated against the performance achieved under a rule-based control (RBC) for a simulated HPWH. A rigorous first principles model shown in Equation 3 describes the temperature stratification in a thermal energy storage tank that was spatially discretized into  $n$  nodes (Nash, Badithela, and Jain 2017). This model is used in this study to predict the thermal dynamics of a HPWH. To model heat transfer from natural convection within the tank when a temperature inversion occurs between nodes, the conduction term is modified based on Equation 4 when a temperature inversion occurs (Nash, Badithela, and Jain 2017).

Equation 3: Temperature dynamics of each node in the HPWH tank model (Nash, Badithela, and Jain 2017)

$$C_p m_i \frac{dT_i}{dt} = \dot{Q}_{cond, i-1} + \dot{Q}_{cond, i+1} + \dot{Q}_{conv, i} + \dot{Q}_{amb, i} + \dot{Q}_{HP, i} + \dot{Q}_{aux, i}$$

where,

$C_p$  is the heat capacity of water

$m_i$  is the mass of water in the  $i$ -th node

$T_i$  is the water temperature in the  $i$ -th node

$\dot{Q}_{cond}$  is the conductive heat transfer rate from the above or below node

$\dot{Q}_{conv}$  is the convective heat transfer rate within the node

$\dot{Q}_{amb}$  is the heat transfer rate to the ambient environment

$\dot{Q}_{HP}$  is the heat pump heat transfer rate into the water

$\dot{Q}_{aux}$  is the electric resistance heater heat transfer rate into the water

Equation 4: Improved conduction term (Nash, Badithela, and Jain 2017)

$$\dot{Q}_{cond, i+1} = \frac{\bar{k}A}{\Delta Z} (T_{i+1} - T_i)$$

$$\bar{k} = \begin{cases} k\Delta(T_i - T_{i+1}), & \text{if } T_{i+1} < T_i \\ k, & \text{otherwise} \end{cases}$$

The stage cost function of the MPC, which is minimized, is formulated as shown in Equation 5.

Equation 5: The stage cost function of the MPC

$$\sum_{k=0}^{N-1} \omega_1 p_{elec,k}(P_{HP,k} + P_{aux,k}) + \omega_2 p_{ghg,k}(P_{HP,k} + P_{aux,k}) + \omega_3 T_{viol,k}$$

where,

$p_{elec,k}$  is the electric tariff at the  $k$ th time step in the prediction horizon,  
 $p_{ghg,k}$  is the forecasted marginal GHG at the  $k$ th time step in the prediction horizon,  
 $P_{HP,k}$  and  $P_{aux,k}$  are the predicted power consumption of the HP and electric resistance heating element at the  $k$ th time step in the prediction horizon, respectively,  
 $T_{viol,k}$  is the violation of the tank water temperature beyond the minimum or maximum bound at the  $k$ th time step, and  
 $\omega_1$ ,  $\omega_2$ , and  $\omega_3$  are the weighing coefficients used to manage the tradeoff between minimizing electricity cost, grid GHG emissions and temperature violations, respectively

To prevent the MPC from trading off temperature violations with reduction in the two other stage cost function terms, a large penalty is placed on the temperature violation. Specifically, the weight value of  $\omega_3 = 2$  is applied. Although outdoor air temperature impacts HP efficiency a constant-efficiency type model is used to calculate the HP power consumption for simplicity.

The MPC uses a prediction horizon of 24 hours to account for a full diurnal cycle. A controller time step of 5 minutes is used to manage tradeoff between control performance and computational complexity of the MPC. In all simulations, a constraint is imposed such that only one heating device may be on at each time step. Both the MPC and RBC prioritize the use of HP over the resistive heating elements. The MPC may choose to turn on the electric resistive heating elements when the HP cannot meet high hot water demand. The RBC turns on the electric resistance heaters when a large enough setpoint difference occurs.

Perfect forecasting of the exogenous inputs of water mass flow rate (based on field data measurements), inlet water temperature (constant over time), ambient temperature surrounding the HPWH, marginal GHG emissions is assumed. The water mass flow rate data was collected from a 2-bedroom unit in a multi-family complex located in California Climate Zone 12. In general, water draw profiles can vary significantly from one household to the next and these simulations are investigating the upper limit for load flexibility in HPWHs based on real-world installations.

A residential TOU electric tariff with a single peak window is used. The peak period occurs from 4pm – 9pm. The peak price is \$0.50/kWh. For off peak, the price is \$0.35/kWh. The effect of varying peak rate is also investigated to study the effect of this parameter on savings potential of the MPC. The minimum and maximum temperature of the MPC is specified to be 42 °C to 50 °C, respectively. This choice is based on the approximate temperature range of the HPWH when it is operated by the RBC with a setpoint of 50 °C and a deadband of 8.33 °C (41.67 °C to 50 °C). The lower temperature range is rounded to 42 °C since the MPC tends to maintain the tank water temperature near the minimum bound for periods to save energy.

Restricting the temperature bounds to a smaller range ensures that the water temperature for both cases is maintained within the range 41.67 °C to 50 °C.

The MPC problem is solved using CPLEX (IBM 2022) with the absolute gap tolerance set at \$0.001 and a maximum solve time of 20 seconds. In all closed-loop simulations, the tank water temperature is initialized at 44 °C (near the lower end of the temperature range) to prompt the heating device to turn on at least once during the simulation. All simulations start at midnight.

## Simulation Results

### One-day simulation results

Several one-day simulation results are presented to analyze the behavior of the HPWH model under MPC and the RBC. All cases considered in this section did not turn on the resistive heating element so only decisions to turn the HP on/off are shown. With exception to one of cases considered in this section, the HPWH tank water temperature is simulated with a one-node model (i.e., a lumped model) meaning that the simulated tank temperature represented an average temperature.

The results for the baseline RBC are shown in Figure 3. The vertical temperature profiles in Figure 3b (as well as for all other temperature profiles presented here) correspond to the upper and lower end of the deadband, respectively. In this case, the RBC turns the HP on twice in the 24-hour period to return the water temperature to setpoint after the water draw events causes the water temperature to decrease below the minimum bound. However, when the HP is turned on the second time, it overlaps with the peak period. The total cost for this 24-hour period is \$0.88. Note that RBC is a reactive controller, such that it responds to water draw events as they occur, unlike MPC that predicts and proactively responds to hot water draws.

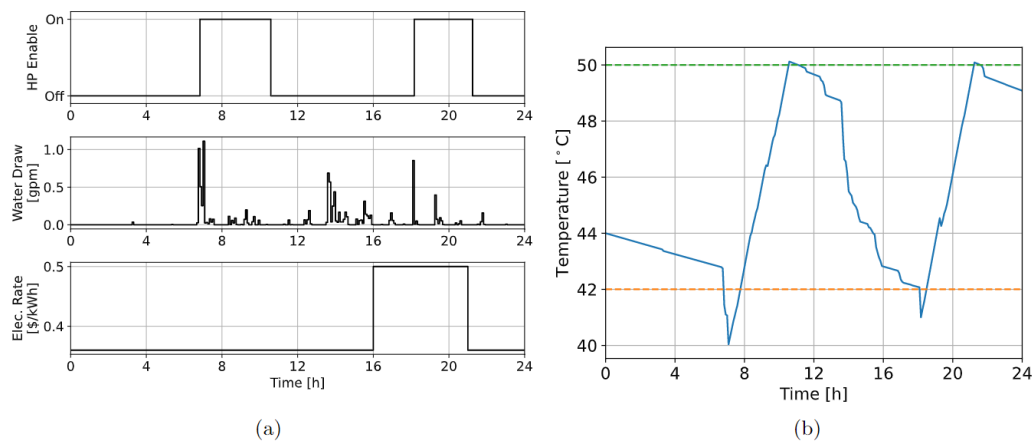


Figure 3: The (a) HP on/off, water draw profile, and electricity rate and (b) average water temperature profile under RBC

Figure 4 shows the results of the MPC in minimizing electricity cost ( $\omega_1 = 1$  and  $\omega_2 = 0$ ). As seen in Figure 4b, the temperature profile in the tank under MPC is noticeably different compared to that under RBC. The MPC benefits from the perfect forecast of the water draw events over the 24-hour period. This preview capability enables the MPC to preheat the water in the tank prior to the large draw event in the morning. The large water draw event causes the

water temperature to drop below the minimum. However, the magnitude of this temperature violation is small compared to that under the RBC. After this period, the tank water temperature is kept near the minimum to save energy and is then heated a little higher before the peak period begins. In this scenario, the total cost was reduced to \$0.51, which is a 42% improvement compared to the operating strategy of the RBC. Looking at the HP on/off chart, it is clear the MPC results in more HP cycling compared to the RBC. This can have negative impacts on equipment lifetime. Constraints are needed, and are later presented, to avoid excessive cycling of HP.

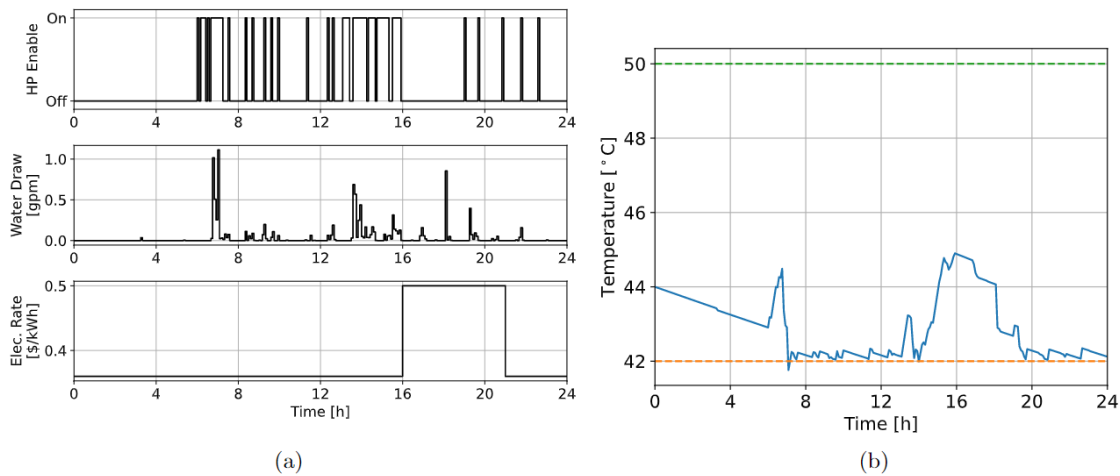


Figure 4: The (a) HP on/off, water draw profile, and electricity rate and (b) average water temperature profile under MPC for cost-optimization only

Due to higher electricity cost in the peak period, one might expect that the MPC would not run the equipment during that time. Figure 5 illustrates the case when the tank water is heated near the upper end of the deadband before the peak period. The resulting cost was \$0.65, which is a 26% improvement compared to the RBC, but is worse than the cost of the previous MPC case. This implies that the MPC in the previous case is balancing minimizing HP use during the peak period and managing energy consumed from pre-heating that could be lost to the ambient. The results suggest that the amount to pre-heat the tank water can be nontrivial and cannot be easily written as a set of rules to generate a schedule for RBC to operate during cheaper TOU periods.

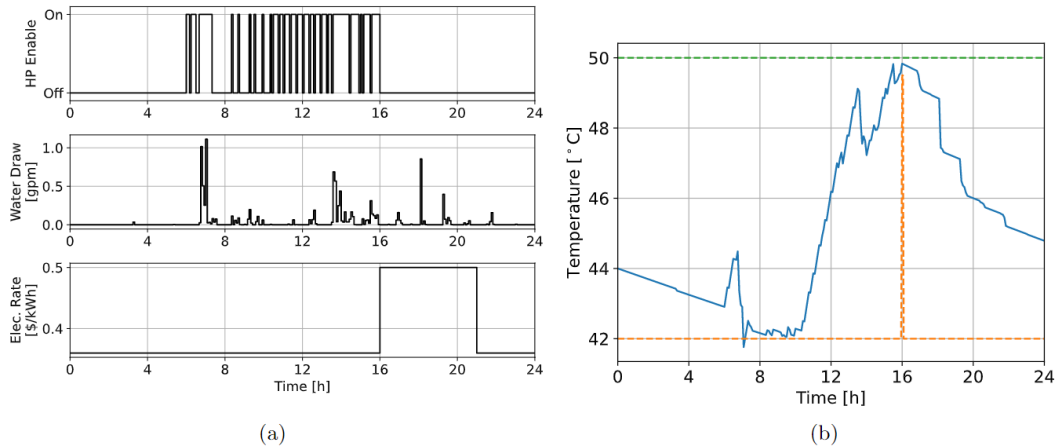


Figure 5: The (a) HP on/off, water profile, and electricity rate and (b) MPC results for control trajectory with no runtime in the peak period

The case shown in Figure 6 considers the situation of model mismatch between the model simulating HPWH behavior and the prediction model of the MPC. In this case, the MPC model is a 1-node tank thermal dynamic model and the HPWH tank is a 12-node model. Overall, the operating behavior is very close to no model mismatch (Figure 4). The cost is \$0.56 with minimal performance degradation observed due to model mismatch.

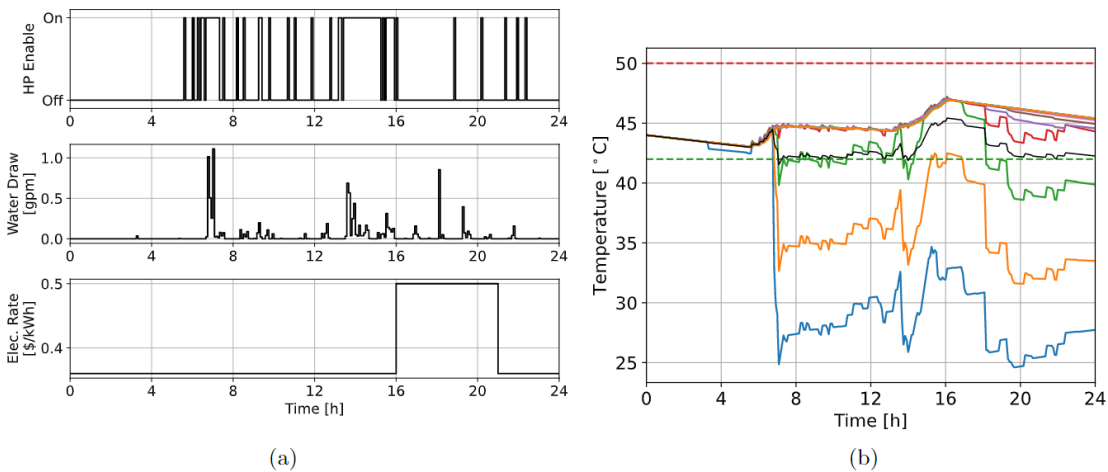


Figure 6: The (a) HP on/off, water profile, and electricity rate and (b) water temperature profiles under MPC for cost-optimization under model mismatch

Figure 7 shows the result for when the MPC controls the HPWH to minimize GHG emissions ( $\omega_1 = 0$  and  $\omega_2 = 1$ ). For the simulated 24-hour period, the margin GHG emissions rate partially mirrors the electricity tariff, but it has a second peak just before midnight. The temperature profile in the tank follows a similar pattern to Figure 4 with a little more usage in the early morning hours when a dip occurs in the GHG data. Overall, while optimizing for GHG, the MPC reduced the HPWH's emissions by 30% compared to the RBC ( $1.20 \times 10^{-3}$  lb versus  $1.72 \times 10^{-3}$  lb). Additionally, the estimated total cost was \$0.54 under MPC for optimizing GHG emissions.

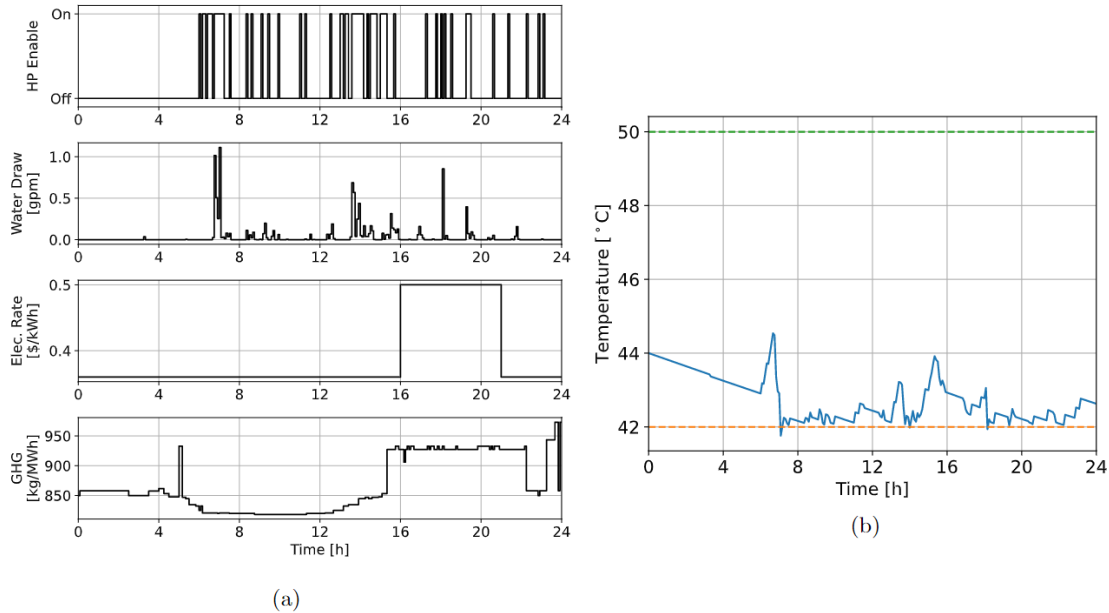


Figure 7: The (a) HP on/off, water profile, and electricity rate and (b) water temperature profiles under MPC for GHG emission optimization only

### Seven-day simulation results

The one-day simulation results show how the operating behavior of the MPC is different from that of the RBC, resulting in lower cost under MPC but with rapid HP cycling. Constraints are needed to enforce a minimum on and minimum off time for the HP. These constraints are called Dwell-time constraints and were added to the MPC. From laboratory experiments with a real HPWH, the minimum on and off time is determined to be 10 min and 5 minutes, respectively.

Two cases are presented in this section: First, the peak rate was varied to analyze benefit of MPC over RBC; Second, the weighing coefficients in the objective function were varied to assess the performance of MPC. Both cases were simulated for the week from Monday, January 3, 2022 at midnight to Monday, January 10, 2022 at midnight. The exogenous inputs is shown in Figure 8.

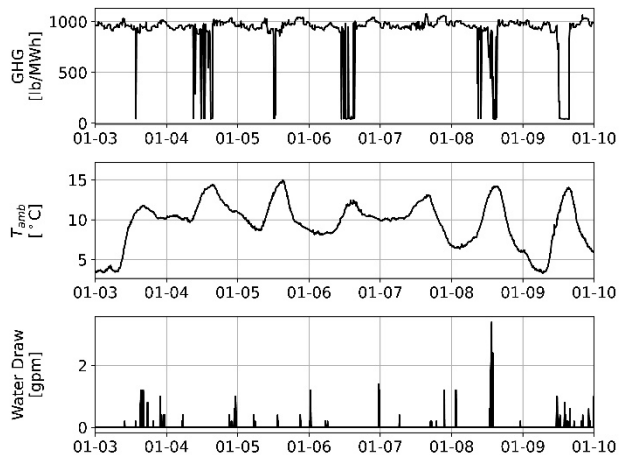


Figure 8: The exogenous input profiles for simulated week

In the case of varying peak rate, the estimated cost and marginal GHG emissions under the MPC ( $\omega_1 = 1$  and  $\omega_2 = 0$ ) and RBC are summarized in Table 1. The key finding is that as the peak rate increases, the benefit of MPC for optimizing cost increases.

Table 1: The estimated cost and marginal GHG emissions of MPC and RBC under varying peak rate for the simulated week

Peak Rate (\$/kWh)	MPC Cost (\$)	RBC Cost (\$)	Improvement (%)	MPC GHG ( $\times 10^{-3}$ lb)	RBC GHG ( $\times 10^{-3}$ lb)	Improvement (%)
0.45	3.84	4.15	7.5	9.02	9.29	2.9
0.50	3.92	4.30	8.8	9.00	9.29	3.1
0.60	3.97	4.61	13.9	8.81	9.29	5.2
0.70	4.09	4.91	16.6	9.09	9.29	2.1
0.80	4.18	5.21	19.8	9.21	9.29	0.8
0.90	4.21	5.51	23.7	9.16	9.29	1.4
1.00	4.22	5.82	27.4	9.08	9.29	2.3

The second case varies the weighing coefficients in the stage cost function of the MPC. The peak rate is fixed at \$0.50/kWh. Table 2 summarizes the estimated cost and marginal GHG emissions under MPC and the RBC. The results indicate a level of trade-off between cost and GHG emissions reduction, but do not generate a clear Pareto front. Depending on the choice of weighing coefficients, the MPC can reduce the cost and GHG emissions compared to the cost and GHG emissions under the RBC.

Table 2: The estimated cost and marginal GHG emissions of MPC with varying weighing coefficient values compared to RBC for one week.

$\omega_1$	$\omega_2$	MPC Cost (\$)	Improvement (%)	MPC GHG ( $\times 10^{-3}$ lb)	Improvement (%)
0.0	1.0	3.57	17.2	6.95	25.2
0.2	0.8	3.90	9.4	7.57	18.6
0.4	0.6	3.87	10.0	7.58	18.4
0.5	0.5	3.94	8.5	7.75	16.6
0.6	0.4	3.90	9.5	7.64	17.7
0.8	0.2	3.90	9.5	7.75	16.6
1.0	0.0	3.83	11.0	8.74	5.9

## Conclusion

Heat pumps for water heating are currently controlled using rule-based logic to maintain a programmed water temperature setpoint. While this approach is proven and robust for maintaining a user-defined setpoint, this type of control does not provide any flexibility as to when the heat pump operates. MPC is an optimization-based predictive control technique that determines control actions through predicting system behavior over a given time horizon and choosing the control actions that optimizes a cost function, which can help reduce the utility costs associated with the electrification of water heating and provides an automated way to meet

customer demand and provide load flexibility. In this simulation study, an economic MPC was formulated using a graph-based control framework that modularized the problem formulation so adaption to different equipment only requires updates to subcomponents and not the whole control architecture. The results for the 24-hour simulations show that with perfect forecasting, MPC can reduce daily equipment operation costs for a simulated HPWH by up to 42%. Additionally, GHG emissions can be reduced by up to 30% while still achieving 35% electricity savings. Moreover, the results for the seven-day simulations show that as peak rate increases, the benefit of using MPC to operate a simulated HPWH increases and that depending on the weights of the multiple objectives in the stage cost function, the MPC can reduce the electricity cost and marginal GHG emissions of the HPWH compared to the RBC.

## Acknowledgements

Funding for the work is provided by California Energy Commission under agreement EPC-19-015.

## References

- CEC (California Energy Commission). 2022. "New Data Indicates California Remains Ahead of Clean Electricity Goals." [www.energy.ca.gov/news/2022-02/new-data-indicates-california-remains-ahead-clean-electricity-goals](http://www.energy.ca.gov/news/2022-02/new-data-indicates-california-remains-ahead-clean-electricity-goals).
- CPUC (California Public Utilities Commission). 2020. "Fact Sheet: Heat Pump Water Heater Incentive Programs." [www.cpuc.ca.gov/-/media/cpuc-website/divisions/energy-division/documents/building-decarb/cpuc-hpwh-and-electrification-fact-sheet\\_q22020.pdf](http://www.cpuc.ca.gov/-/media/cpuc-website/divisions/energy-division/documents/building-decarb/cpuc-hpwh-and-electrification-fact-sheet_q22020.pdf).
- Delforge, P. and J. Vukovich. 2018. *Can Heat Pump Water Heaters Teach the California Duck to Fly?* Pacific Grove, CA: ACEEE. [www.aceee.org/sites/default/files/pdfs/Can-Heat-Pump-Water-Heaters-Teach-the-California-Duck-to-Fly.pdf](http://www.aceee.org/sites/default/files/pdfs/Can-Heat-Pump-Water-Heaters-Teach-the-California-Duck-to-Fly.pdf).
- Delforge, P. 2020. "Heat Pump Water Heaters as Clean-Energy Batteries." Natural Resources Defense Council, January 7. [www.nrdc.org/experts/pierre-delforge/heat-pump-water-heaters-clean-energy-batteries](http://www.nrdc.org/experts/pierre-delforge/heat-pump-water-heaters-clean-energy-batteries).
- EIA (Environmental Impact Assessment). 2018. "Space heating and water heating account for nearly two thirds of U.S. home energy use." [www.eia.gov/todayinenergy/detail.php?id=37433#](http://www.eia.gov/todayinenergy/detail.php?id=37433#).
- Ellis, M., H. Durand, and P.D. Christofides. 2014, "A tutorial review of economic model predictive control methods." *Journal of Process Control*, 24: 1156-1178.
- IBM (2022). IBM ILOG CPLEX Optimizer. [www.ibm.com/analytics/cplex-optimizer](http://www.ibm.com/analytics/cplex-optimizer).
- Jin, X., J. Maguire, and D. Christensen. 2014. *Model Predictive Control of Heat Pump Water Heaters for Energy Efficiency*. Pacific Grove, CA: ACEEE. [www.aceee.org/files/proceedings/2014/data/papers/1-296.pdf](http://www.aceee.org/files/proceedings/2014/data/papers/1-296.pdf).

Nash, A. L., A. Badithela, and N. Jain. 2017. “Dynamic modeling of a sensible thermal energy storage tank with an immersed coil heat exchanger under three operation modes.” *Applied Energy* 195: 877–889.

Rawlings J.B., D.Q. Mayne, and M.M. Diehl. 2019. *Model Predictive Control: Theory, Computation, and Design, 2nd ed.* Santa Barbara, CA: Nob Hill Publishing.

Wanjiru, E.M., S.M. Sichilalu, and X. Xia. 2017. “Model predictive control of heat pump water heater-instantaneous shower powered with integrated renewable grid-energy systems.” *Applied Energy* 204: 1333-1346.